Formation of longitudinal structures in granular flows

Igor S. Aranson[1] and Lev S. Tsimring[2]
[1] *Argonne National Laboratory, 9700 South Cass Avenue, Argonne, IL 60439*
[2] *Institute for Nonlinear Science, University of California, San Diego, La Jolla, CA 92093-0402*
(February 1, 2008)

In the framework of the theory of partially fluidized granular flows we study the formation of longitudinal structures observed experimentally by Forterre and Pouliquen in a flow down a rough inclined plane. We show that the formation of longitudinal structures is related to the positive feedback between the fluidization rate and the lateral stress (side pressure), which leads to a convective instability. Our theory explains main experimental features, such as appearance and amplification of the structure at some distance from the outlet and non-stationary behavior of the structures.

PACS: 45.70.-n, 45.70.Ht, 45.70.Qj, 83.70.Fn

The dynamics of granular media has been an active area of research for physicists [1] and engineers [2]. One of the most interesting phenomena pertinent to many granular systems is the transition from a static equilibrium to a granular flow. There has been a number of experimental studies of flows in large sandpiles [3,4] as well as in thin layers of grains on inclined surfaces [5–8]. Recent experiments with granular flows on a rough inclined plane revealed a new striking phenomenon: formation of non-stationary longitudinal structures at some distance downstream from an outlet [8]. Authors of [8] proposed an explanation of the instability mechanism based on analogy with thermal convection in fluids: a rapid shear granular flow leads to the increase of the granular temperature near the rough bottom. Because of the intrinsic dissipative nature of collisions between particles, the granular temperature should decay away from the bottom, creating necessary conditions for the "thermal granular convection" (cf. [10,11]). Using hydrodynamic equations obtained from the kinetic theory for dilute granular gases, this instability was studied analytically and numerically [9]. Although shear flow activated thermal granular convection could be a useful concept for the interpretation of experimental results, the theory [9] did not address two important observations: (1) experiments as well as simulations [12] show that fluctuations of velocity are more significant near the free surface of the granular flow, and so the granular temperature may in fact be higher at the top rather than at the bottom, (2) longitudinal structures appear at some distance downstream from the outlet and exhibit complex spatio-temporal dynamics.

In this Letter we demonstrate that the observed transverse instability can be described within the framework of the continuum theory of partially fluidized flows proposed by us in Refs. [13,14] without invoking the concept of granular temperature more appropriate for dilute gas-like granular flows. In this theory, we introduce an equation for the order parameter which characterizes the phase state of the granular matter. In a certain range of parameters, the shear flow described by these equations, is unstable with respect to transverse perturbations. We show that this instability is of convective nature, i.e. small perturbations grow downstream while remaining small in the laboratory frame. Thus, the "rolls" appear at some finite distance from the outlet. This distance depends on the noise level and flow conditions. Since the pattern structure is determined by random fluctuations near the outlet, the resulting pattern is always non-stationary in the laboratory frame, very similar to that observed experimentally.

Model. The starting point of our theory is the momentum conservation equation

$$\rho_0 Dv_i/Dt = \frac{\partial \sigma_{ij}}{\partial x_j} + \rho_0 g_i, \quad j = 1, 2, 3. \tag{1}$$

where v_i are the components of velocity, $\rho_0 = const$ is the density of material (in the following we set $\rho_0 = 1$), $\mathbf{g}$ is acceleration of gravity, and $D/Dt = \partial_t + v_i \partial_{x_i}$ denotes the material derivative. Since the relative density fluctuations are small, the velocity obeys the incompressibility condition $\nabla \cdot \mathbf{v} = 0$. The stress tensor is represented as a sum of the hydrodynamic part proportional to the flow strain rate and the strain-independent part,

$$\sigma_{ij} = \eta \left(\frac{\partial v_i}{\partial x_j} + \frac{\partial v_j}{\partial x_i} \right) + \sigma^s_{ij}, \tag{2}$$

where η has the meaning of the viscosity coefficient. At this point we introduce the order parameter (OP) ρ which describes the "phase state" of the granular matter: it varies from 0 in the "liquid" phase to 1 in the "solid" phase. We interpret the OP as the relative local density of static contacts among the grains. In the solid state ($\rho = 1$) the strain-independent part should coincide with the "true" static stress tensor σ^0_{ij} for the immobile grain configuration in the same geometry, and in the completely fluidized state ($\rho = 0$) we should have $\sigma^s_{ij} = -\Pi \delta_{ij}$ (Π is the hydrodynamic pressure). According to our assumption, the off-diagonal elements of the strain-independent part of the stress tensor obey the conditions $\sigma^s_{ij} = \rho \sigma^0_{ij}$ for $i \neq j$. In the solid state the normal

stresses σ^0_{ii} do not in general coincide. For the weakly-fluidized state ($\rho \to 1$) the normal stresses are close to the static values, however some dependence on the order parameter ρ (i.e. degree of fluidization) may appear. In the first order in $1-\rho$ one writes for the diagonal elements of the stress tensor

$$\sigma^s_{ii} = \sigma^0_{ii} + \alpha_i(1-\rho) + O((1-\rho)^2) \tag{3}$$

where α_i characterizes the response of the normal stresses on fluidization. Since fluidization is accompanied by the decrease in the number of static contacts among granules (i.e. dilution), the normal stresses should decrease with fluidization, i.e. $\alpha_i > 0$. It also agrees with the observation in Ref. [8] that the crests of the surface deformations correspond to a more dilute granular state.

According to Ref. [13,14], the equation for the order parameter ρ is taken in the form

$$\dot\rho + v\nabla\rho = \nabla^2\rho + \rho(1-\rho)(\rho-\delta), \tag{4}$$

where $\delta = (\phi-\phi_0)/(\phi_1-\phi_0)$ is the control parameter, $\phi = \max|\sigma^0_{mn}/\sigma^0_{nn}|$ is the maximum ratio of shear to normal stresses in the bulk, and $\tan^{-1}\phi_{1,2}$ are static and dynamic repose angles characterizing the granular material. Parameter ϕ which enters the Mohr-Coloumb yield condition [2], in the context of our theory is equivalent to a melting temperature in the theory of phase transition.

Following the analysis of Ref. [13], we consider a layer of dry cohesionless grains on an inclined rough surface (see Fig.1). However, now we assume that the layer thickness h can vary in both x and y directions. The momentum conservation equation (1) in the stationary regime yields the force balance conditions

$$\sigma_{xz,x} + \sigma_{yz,y} + \sigma_{zz,z} = g\cos\varphi, \tag{5}$$
$$\sigma_{xx,x} + \sigma_{xy,y} + \sigma_{xz,z} = -g\sin\varphi, \tag{6}$$
$$\sigma_{xy,x} + \sigma_{yy,y} + \sigma_{yz,z} = 0, \tag{7}$$

where the subscripts after commas mean partial derivatives, and $z=0$ corresponds to the bottom of the layer. We assume that variations of the layer thickness along the y direction are small. Accordingly, there will be a small component of velocity along y direction and corresponding stress components σ_{yz} and σ_{yy}. In the avalanche problem considered in Ref. [13] these terms were irrelevant. We show later that the transverse flux is crucial for the explanation of longitudinal structures.

In the first order in h_x, h_y Eqs. (5)-(7) yield

$$\sigma_{zz} \approx g\cos\varphi(z-h)\ ,\ \sigma_{xz} \approx -g\sin\varphi(z-h),$$
$$\sigma_{yz} = \int_z^h dz\sigma_{yy,y}. \tag{8}$$

Here we used the conditions $\sigma_{xx} = const, \sigma_{xy} = const$ and $\sigma_{zz} = \sigma_{xz} = \sigma_{yz} = 0$ on free surface $z = h$.

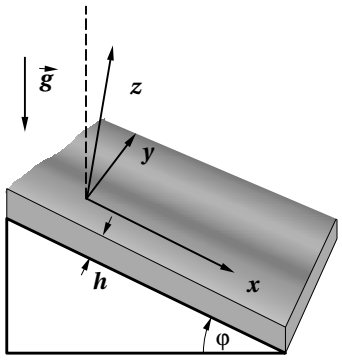

FIG. 1. Schematic representation of a chute geometry. z-axis is normal to the chute bottom, dashed line is parallel to the direction of gravity.

For the chute geometry Fig. 1 parameter δ in Eq. (4) can be specified. For $h = const$ there is a simple relation between shear and normal stresses, $\sigma_{xz} = -\tan\varphi\sigma_{zz}$. The most "unstable" yield direction is parallel to the inclined plane, i.e. $\phi = |\sigma_{xz}/\sigma_{zz}|$ and $\delta = \delta_0 = (\tan\varphi - \phi_0)/(\phi_1-\phi_0)$. If h is a slowly varying function of x and y, one obtains for the parameter δ:

$$\delta = \delta_0 - \beta h_x + O(h_x^2, h_y^2) \tag{9}$$

where $\beta = 1/(\phi_1-\phi_0)$ (see [13,14] for more details).

Thin layer solutions of Eq. (4) for the chute geometry Fig. 1 are subject to the following boundary conditions (BC): no-flux condition $\rho_z = 0$ at the free surface $z = h$, and no-slip condition $\rho = 1$ at the bottom of the chute $z = 0$ (a granular medium is assumed to be in a solid phase near the rough surface). The velocity profiles corresponding to a stationary profile of $\rho(z)$, can be easily found from Eq. (2),(3),

$$\eta\frac{\partial v_x}{\partial z} = -g\sin\varphi(z-h) - \rho\sigma^0_{xz} = -g\sin\varphi(1-\rho)(z-h),$$
$$\eta\frac{\partial v_y}{\partial z} = -\int_z^h \alpha_y\partial_y\rho dz \tag{10}$$

In the derivation of Eq. (10) we used $\sigma^s_{yz} = 0$ for a flat layer. The components of the flux $\mathbf{J} = \int_0^h \mathbf{v}(z)dz$ are

$$J_x = -\frac{g\sin\varphi}{\eta}\int_0^h dz\int_0^z (1-\rho(z'))(z'-h)dz'$$
$$J_y = -\frac{\alpha_y}{\eta}\int_0^h dz\int_0^z dz''\int_{z''}^h \partial_y\rho dz' \tag{11}$$

For thin weakly-fluidized layers (see [13,14]), we can look for solution of Eq.(4) in the form

$$\rho = 1 - A\sin\left(\frac{\pi}{2h}z\right) + \text{h.o.t.}, \tag{12}$$

where $A \ll 1$ is a slowly varying function of t, x, and y. Substituting ansatz (12) into Eq. (4) and applying orthogonality conditions [13,14]), we obtain

$$A_t = \Lambda A + \nabla_\perp^2 A + \frac{8(2-\delta)}{3\pi} A^2 - \frac{3}{4} A^3 - \bar{\mu} h^2 A \partial_x A \quad (13)$$

where $\nabla_\perp^2 = \partial_x^2 + \partial_y^2$, $\Lambda = \delta - 1 - \frac{\pi^2}{4h^2}$, $\bar{\mu} = (3\pi^2 - 16) g \sin\varphi / 3\pi^3 \eta = 0.146 g \sin\varphi/\eta$. The mass conservation yields

$$\frac{\partial h}{\partial t} = -\nabla \cdot \mathbf{J} = -\partial_x J_x - \partial_y J_y \quad (14)$$

where the flux components $J_{x,y}$ calculated from Eq. (11) in the thin layer approximation, are

$$J_x = \mu h^3 A \; , J_y = -\alpha_1 h^2 A h_y + \alpha_2 h^3 A_y \quad (15)$$

$\mu = 2(\pi^2 - 8) g \sin\varphi / \eta \pi^3 \approx 0.12 g \sin\varphi/\eta$, $\alpha_1 = \alpha_y(\pi^3 + 8\pi - 48)/2\pi^3\eta \approx 0.13\alpha_y/\eta$, $\alpha_2 = 8\alpha_y/\pi^3\eta \approx 0.26\alpha_y/\eta$.

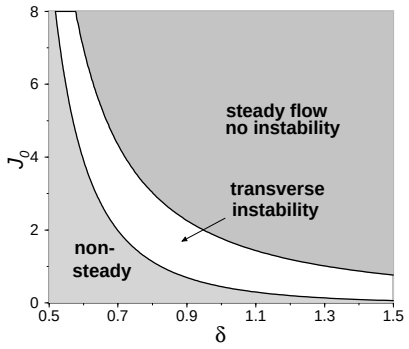

FIG. 2. Phase diagram in $\delta - J_0$ plane.

Our model has two control parameters, the downhill mass flux J_0 at the outlet $x = 0$, and δ. For large enough J_0 and δ, Eqs. (13),(14) possess a steady-state solution $A = A_0, h = h_0$ (see Fig.2). The stability of this solution can be examined by substituting the ansatz $\{A, h\} = \{A_0, h_0\} + \{\zeta, \xi\} \exp(\lambda t + i k_x x + i k_y y)$, where $\{\zeta, \xi\}$ is a small perturbation. For long-wave perturbations ($k_x, k_y \ll 1$) in the leading order one obtains for the growth rate λ

$$\lambda = i k_x \mu h_0^2 A_0 + B k_y^2 + ... \quad (16)$$

where $B = \pi^2 \alpha_2 [16(2-\delta)/3\pi - 3A_0]^{-1} - \alpha_1 h_0^2 A_0$. As seen from Eq. (16), pure longitudinal perturbations $k_y = 0$ are neutrally stable, but for $B > 0$ the perturbations with transverse component of the wave number can be unstable. For pure transverse perturbations ($k_x = 0$) the instability is aperiodic (λ is real), as in thermo-convection in ordinary fluids. The physical meaning of the instability is the following: decrease of ρ (increase of fluidization) corresponds to the decrease of the lateral pressure ($-\sigma_{yy}$) which in turns lead to the increase of the height h and further fluidization. The phase diagram of the instability on $\delta - J_0$ plane is shown in Fig. 2. The transverse instability exists in the band restricted from above by the condition $B = 0$ and from below by the existence of steady-state solution [19].

Complexity of λ and asymmetry of the problem in x-direction signal the possibility of the convective nature of the instability: the perturbations may grow in the moving frame and decay in the laboratory frame (see, e.g. [15,16]). As a test for convective instability one has to examine the value of λ for the saddle point of the function $\lambda(k_x, k_y)$ in the complex k_x plane, i.e. $\partial\lambda/\partial k_x = 0$. In fact, it is easy to see that if the instability is weak (for $\alpha_y \ll 1$) and the downhill flux J_0 is finite, the instability has to be convective. In the presence of persistent fluctuations, e.g. at the flow outlet, the perturbation will be spatially amplified down the flow.

Let us estimate the spatial growth rate. Consider the unstable perturbations caused by a small stationary y-periodic force with wavenumber k_0 localized at $x = 0$. Calculations show that the linearized solution ζ will be described by the integral

$$\zeta \sim \int_{-\infty}^{\infty} \exp[i\mathbf{kr}] \frac{dk_x}{\lambda(\mathbf{k})} \left(1 - \exp[\lambda(\mathbf{k})t]\right) \quad (17)$$

The non-stationary part $\sim \exp[i\lambda(\mathbf{k})t]$ decays in time due to the convective character of the instability, and the integral yields

$$\zeta \sim \exp[i k_0 y + i k^* x] \quad (18)$$

where k^* is found from $\lambda(k_x = k^*, k_0) = 0$. It is easy to see from Eq.(16) that, for small k^0, $k^* \approx -iBk_0^2/\mu h_0^2 A_0$. Since k^* is imaginary, perturbations from a stationary source at $x = 0$ grow exponentially downhill. For random perturbations introduced at the outlet the typical scale of the pattern will be determined by the most unstable wavenumber in the transverse direction. However, the pattern will remain non-stationary due to intrinsically random nature of the noise.

We studied Eqs. (13),(14) numerically. The simulations were performed in a large system, more than 2000 dimensionless units in x-direction (downhill), and 200 units in y-direction. Fixed flux boundary conditions were imposed at the outlet at $x = 0$. Selected results are presented in Figs. 3,4. Figure 3 illustrates spatial amplification of perturbations downstream and formation of longitudinal structures. As it follows from our simulations, far away from the outlet the structures remain non-stationary and exhibit spatio-temporal dynamics which are very similar to observed in Ref. [8]. The profiles of h and A vs y are shown in Fig. 4. In agreement with experiment, crests in h corresponds to crests in A, i.e. to more fluidized regions of flow.

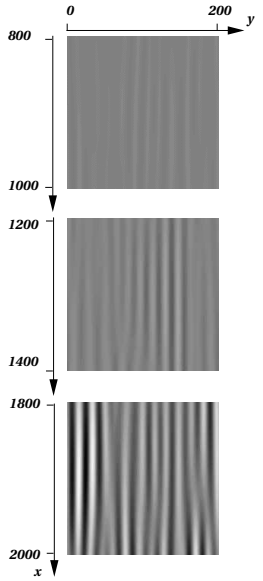

FIG. 3. Grey-scale snapshots of $h(x,y)$ (white corresponds to larger h), for $\delta = 1.5$, $\mu = 0.025$, $\beta = 3.14$, $J_0 = 1.75$, $\alpha_y = 0.04$. Equilibrium value of the layer thickness $h_0 \approx 4.45$.

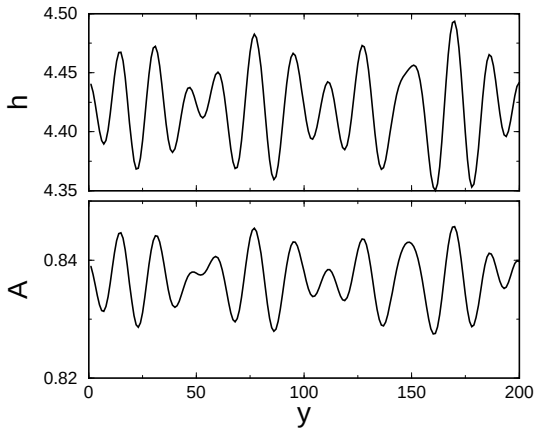

FIG. 4. Profiles of $h(y)$ and $A(y)$ at $x = 2000$.

We demonstrated that formation of longitudinal structures in granular flow down a rough inclined plane is the result of noise amplification and saturation due to the convective instability. The mechanism of the instability is related to the dependence of the local pressure on the fluidization rate controlled by the order parameter. We conjectured a simple linear relation between these quantities. It would be of interest to verify this relation in physical experiment and molecular dynamic simulations. The convective character of the instability suggests that the flow can be controlled by small systematic perturbations introduced at the outlet.

In recent paper [20], a novel fingering instability in a thin granular layer inside a horizontal rotating cylinder was reported. We believe that the nature of this instability fundamentally is the same as described here. The only important difference is that due to backflow the perturbation can propagate upstream, and thereby the convective instability becomes "global". This may explain why this fingering instability occurs in a "short" system as compared with inclined layer experiment [8].

This research was supported by the Office of the Basic Energy Sciences at the US DOE, grants W-31-109-ENG-38 and DE-FG03-95ER14516. Simulations were performed at the National Energy Research Scientific Computing Center.

[1] H.M. Jaeger, S.R. Nagel, and R.P. Behringer, Rev. Mod. Phys. **68**, 1259 (1996); L. Kadanoff, Rev. Mod. Phys. **71**, 435 (1999); P. G. de Gennes Rev. Mod. Phys. **71**, S374 (1999).

[2] R.M. Nedderman, *Statics and Kinematics of Granular Materials*, (Cambridge University Press, Cambridge, England, 1992)

[3] R.A. Bagnold, Proc. Roy. Soc. London A **225**, 49 (1954); *ibid.*, **295**, 219 (1966)

[4] J. Rajchenbach, in *Physics of Dry Granular Media*, eds. H. Hermann, J.-P. Hovi, and S. Luding, p. 421, (Kluwer, Dordrecht, 1998);

[5] A. Daerr and S. Douady, Nature (London) **399**, 241 (1999)

[6] A. Daerr, Phys. Fluids **13**, 2115 (2001)

[7] O. Pouliquen, Phys. Fluids, **11**, 542 (1999)

[8] Y. Forterre and O. Pouliquen, Phys. Rev. Lett. **86**, 5886 (2001)

[9] Y. Forterre and O. Pouliquen, cond-mat/0108517.

[10] R.D. Wildman, J.M. Huntley, and D.J. Parker, Phys. Rev. Lett. **86**, 3304 (2001)

[11] X. He, B. Meerson and G. Doolen, Phys. Rev. E **65** 030301(R) (2002)

[12] L.E. Silbert et al, Phys. Rev. E **64**, 051302 (2002).

[13] I.S. Aranson and L.S. Tsimring, Phys. Rev. E. **64**, 020301 (R) (2001)

[14] I.S. Aranson and L.S. Tsimring, cond-mat/0109358

[15] L.D.Landau and E.M.Lifshitz, *Physical Kinetics*, Pergamon Press, New York, 1981

[16] I.S. Aranson, L. Aranson, L. Kramer, and A. Weber, Phys. Rev. A **46**, 2992 (1992)

[17] J.P. Wittmer, M.E. Cates, and P.J. Claudine, J. Phys. II France **7**, 39, (1997); L. Vanel et al, Phys. Rev. Lett. **84**, 1439 (2000)

[18] M.E. Cates et al, Phys. Rev. Lett. **81**, 1841 (1998)

[19] Our phase diagram is somewhat different from that in Ref. [8] shown in opening width h_g - angle variables. However, the direct comparison is difficult because the opening h_g in Ref. [8] is not explicitly related to the flux J_0. According to Ref. [8] significant variation in h_g practically does not change the stationary thickness of the flow h, and, therefore, J_0.

[20] A. Q. Shen, Phys. Fluids, **14**, 462 (2002).